

Comparative Proteomic Analysis in Left Ventricular Remodeling following Myocardial Infarction in Rats

GU Hong Juan^{1, #}, GAO Chang Bin¹, GONG Jun Li², LI Xiang Jun³, SUN Bo³, and LI Xi Ning³

1. China-Japan Union Hospital of Jilin University, Changchun 130021, Jilin, China; 2. Changchun Municipal Central Hospital, Changchun 130051, Jilin, China; 3. Jilin University College of Pharmacy, Changchun 130021, Jilin, China

Abstract

Objective Left ventricular remodeling (LVR) following myocardial infarction (MI) is a key pathophysiological process in which MI develops into heart failure. The exact mechanism of LVR remains unclear. We performed differential proteomic analysis on the myocardia of rats with LVR after MI, to explore the mechanism of ventricular remodeling after MI.

Methods In the LVR group ($n=12$), after the anterior descending coronary artery was ligated, the rats were fed for four weeks before the LVR models were established. Rats in the sham-operated group ($n=11$) underwent thread-drawing without ligation. The hemodynamic parameters, pathological findings, and proteomics were compared between the two groups.

Results In the LVR group, the left ventricular end-diastolic pressure increased, the maximal left ventricular pressure increase/decrease ratio decreased significantly, and the left ventricular systolic pressure decreased. H-E staining and Masson staining of cardiac muscle tissues of the LVR group showed myocytolysis, disarray, and collagen proliferation. Twenty-one differentially expressed proteins were detected by proteomic analysis. We validated two proteins using western blot analysis. The differentially expressed proteins could be divided into six categories: energy metabolism-related proteins, cytoskeletal proteins, protein synthesis-related proteins, channel proteins, anti-oxidation-related proteins, and immune-related proteins.

Conclusion These differentially expressed proteins might play key roles in LVR following MI.

Key words: Comparative proteomics; Liquid chromatography-mass spectrometry; Left ventricular remodeling; Myocardial infarction; Western blot

Biomed Environ Sci, 2012; 25(1):117-123 doi: 10.3967/0895-3988.2012.01.017 ISSN:0895-3988

www.besjournal.com/fulltext

CN: 11-2816/Q

Copyright ©2012 by China CDC

INTRODUCTION

Acute myocardial infarction (AMI) is a common, life-threatening disorder in clinical practice. Heart failure after myocardial infarction (MI), a common complication of MI, is characterized by high mortality and poor prognosis. Left ventricular remodeling (LVR) is the underlying mechanism of heart failure after MI^[1-2]. LVR following MI refers to the condition in which the

cells, molecules, and inter-cellular substances of the whole left ventricle (LV) change after AMI, followed by changes in the size, morphology, and function of the LV. It can be divided into early (within six weeks) and late stages (six weeks to one year). The possible mechanisms of ventricular remodeling include hemodynamic change, inflammatory reaction, neuroendocrine activation, and apoptosis^[3]. Nevertheless, LVR is a complex issue, and remains a hot topic in cardiovascular research. In this study, by

[#]Correspondence should be addressed to: GU Hong Juan, Tel: 86-431-88948647, 15843086157. E-mail: zhouqiwei777@sina.com
Biographical note of the first author: GU Hong Juan, female, born in 1972, Ph.D candidate, majoring in heart failure.

Received: June 1, 2011;

Accepted: July 11, 2011

establishing animal models, we analyzed the hemodynamics, pathology, and comparative proteomics of LVR following MI, in an attempt to explore its possible mechanism and provide targets for drug therapies.

The term “proteome” was proposed by Wilkins and Williams in 1994. It refers to all the proteins that can be expressed by genes, i.e., all the proteins that are expressed by cells, tissues, or body in a certain time and space^[4]. Proteomics is at the frontier of modern science and technology. It provides a global perspective for understanding the rules of life and many key pathophysiological phenomena. Comparative proteomics is an important component of proteomics. It tries to identify the pathophysiological mechanisms of diseases by comparing and analyzing differentially expressed proteins, and thus provides valuable information for diagnosis, medical treatment, and prognosis. Liquid chromatography-mass spectrometry (LC-MS) is most commonly used for the proteomic analysis of complex samples, because of its very high peak capacity, sensitivity, and speed. Proteomics has been widely applied in clinical subjects, such as tumors and aging. Cardiovascular diseases (CVDs) represent a new field in which proteomics can be applied^[5]. Using proteomic technology, the changes in CVD-related proteins can be dynamically analyzed. It has been speculated that proteomics can provide strong support for the early diagnosis and active treatment of CVD^[6-7]. Proteomics has been applied for research on myocardopathies^[8-9]; however, few studies have focused on LVR following MI.

MATERIALS AND METHODS

Reagents and Experimental Animals

Reagents, including urea, thiourea, Tris, DTE, phenylmethylsulfonyl fluoride, ammonium bicarbonate (NH₄HCO₃), 0.1% formic acid, dithiothreitol (DTT), iodoacetamide, trypsinogen, and methyl cyanides (ACN), were purchased from Sigma (St. Louis, MO, USA). Benzonase DNase and RNase were purchased from Merck (Germany). Antibodies against *Elongation factor 1-alpha1*, *Junction plakoglobin (JUP)*, and *GAPDH* were from Santa Cruz (Santa Cruz, CA, USA). The experimental *Wistar* rats were purchased from the Animal Experiment Center of Jilin University.

Establishment of Animal Models

Twenty-three 10-week-old male *Wistar rats*, weighing 200-250 g, were randomized into the LVR

group ($n=12$) and the sham-operated group ($n=11$). In the LVR group, after the anterior descending coronary artery was ligated, the rats were fed for four weeks before the LVR models were established according to the literature^[10]. Electrocardiograms immediately after the operation and at 24 h showed ST-elevated MI among rats that survived the procedure. Rats in the sham-operated group underwent the same surgical procedure, including thread-drawing, but not ligation, at the same site. Penicillin was given daily at a dose of 240 000 units/kg for three consecutive days to prevent post-operative infections. Both groups were fed under the same dietary regime for four weeks.

Detection of Hemodynamic Parameters

Four weeks after the operation, the rats were anesthetized with chloral hydrate, and a cardiac catheter was inserted into the LV via the right carotid artery and connected with a polygraph. Thus, the left ventricular systolic pressure (LVSP), the left ventricular end-diastolic pressure (LVEDP), and the maximal left ventricular pressure increase/decrease ratio ($\pm dp/dt_{max}$) could be recorded.

Pathological Detection

After the hemodynamic parameters had been completely recorded, the rats were sacrificed and LVs were harvested. LVs were divided into three parts from ligation site to apex. The part that was close to the ligation site was fixed in 12% buffered formalin, embedded in paraffin, sectioned, stained with hematoxylin and eosin (H-E) and Masson dye, and pathologically analyzed. The neighboring parts were preserved in a -80 °C freezer. Eight specimens in the LVR group and seven specimens in sham-operated group were obtained for proteomic analysis. Myocardium from the apex of the heart was reserved for western blotting.

Preparation of Protein Samples

The frozen biopsies were washed with phosphate-buffered saline in sterile Petri dishes to remove any adhering hemoglobin and other proteins originating from hemolysis at the time of sample collection. The tissues were then cut into 1 mm³ pieces, ground into powders in liquid nitrogen, and dissolved in lysis buffer consisting of 7 mol/L urea, 2 mol/L thiourea, 2% (w/v) CHAPS, 50 mmol/L Tris, and 50 mmol/L DTE, 1 mmol/L phenylmethylsulfonyl fluoride, and 1 µg/mL of protease inhibitors cocktail. Benzonase DNase and RNase were added to remove

DNA and RNA. Samples were centrifuged for 1 h at 100 000 g to remove any particulate materials. The protein concentration of sample was measured by the Bradford method^[11]. All samples were stored at -80 °C until use.

Protein Digestion

Before digestion, the samples were diluted with 25 mmol/L NH_4HCO_3 to ensure that the concentration of urea was lower than 2 mol/L. Prior to digestion, the samples were reduced with 20 mmol/L DTT at 56 °C for one hour, and then alkylated with 50 mmol/L iodoacetamide at room temperature in the dark for 30 min. Finally, trypsinogen (sequencing grade), at a ratio of 1:50, was added to the samples and digestion allowed to proceed at 37 °C overnight. After digestion, the samples were vacuum-dried and preserved at -80 °C.

Analysis with LC-MS

The samples were dissolved with buffer A (0.1% formic acid), and then analyzed by LC-MS. The loading volume was 2 µg for each assay. The reversed-phase column was 150×0.1 mm (Michrom). The samples were eluted with 5%-30% buffer B (0.1% formic acid and 99.9% methyl cyanide) at a flow rate of 500 nL/min for two hours. Each sample was tested three times. The reverse phase chromatography-eluted polypeptides were detected using an LTQ Orbitrap mass analyzer (Thermo Scientific) at a mass charge ratio (m/z) of 300-2 000 amu. MS2 scans were performed in a data-dependent manner (20 MS2 scans after each full scan; parent ion m/z width: 3 amu; 35% collision energy; dynamic exclusion time: 30 s).

Data Processing

Spectra with an intensity higher than one unit and over 10 ion signals were searched against a protein database, using the SEQUEST algorithm and Bioworks 3.3.1 SP1 software (Thermo Scientific), to identify the corresponding polypeptides and proteins. The protein database used was the rat protein database (version 3.78), downloaded from the website of the European Bioinformatics Institute (<http://www.ebi.ac.uk/PI/>). The search parameters were as follows: error range of polypeptide mass, 10 ppm; cysteine modification, +57; and two miss-cleaved tryptic sites allowed in partial digestive products. The false positive rate was controlled below 1% in this study to ensure the reliability of the data.

The abundance of each protein was assessed using the spectrum count obtained from three assays. For proteins whose abundance varied among different samples, the changes in the spectrum count must have met the following two conditions: 1) the ratio of the spectrum count of the protein between two samples must be greater than or equal to 1.5. 2) The difference of the spectrum count of the protein between two samples must be greater than or equal to 18 (mean difference between two assays: 6). Multiple comparisons were performed for data obtained from these three assays for each sample to evaluate the false positive rate of the above method in the identification of protein abundance. The false positive rate was found to be 2.31%.

Western Blot Analysis

One hundred milligrams of frozen myocardial tissue at -80 °C was cut off with a sterile blade and placed into a homogenizer. One milliliter of cell lysis buffer was added, and the sample was fully ground on ice (30 min). The ground suspension was transferred into a 1.5 mL EP tube and centrifuged at 12 000 g for five minutes. The supernatant (800 µL) was transferred into another 1.5 mL EP tube, 200 µL 5× sample buffer was added, and the mixture was boiled for five minutes. The sample was then centrifuged at 12 000 g for five minutes and stored at -20 °C. The prepared samples were separated by SDS-PAGE and transferred to PVDF membranes (Bio-Rad). Membranes were blocked in TBST, 0.5% Tween-20 (Fisher) containing 5% skimmed milk, and incubated overnight at 4 °C with the corresponding primary antibodies (*Elongation factor 1-alpha1*, 1:500; *Junction plakoglobin*, 1:500; and *GAPDH*, 1:1 000). Adding secondary antibody (1:5 000 dilution) incubated for 2 h. The immunoblot signals were visualized using the Immobilon Western Chemilum HRP Substrate (WBKLS0100; Millipore Corporation, Billerica, MA, USA). The expression levels of *Elongation factor 1-alpha1* and *Junction plakoglobin* protein relative to the *GAPDH* control were determined by densitometric scanning (Tanon Gel Image system-1 600, Shanghai, China).

Statistical Analysis

The experimental data were expressed as $\bar{x} \pm s$, and were analyzed using SPSS 16.0 software. Student's *t* test was performed, and a *P* value of less than 0.05 was regarded as statistically significant.

RESULTS

Changes in Hemodynamic Parameters

Compared with the sham-operated group, the

hemodynamic parameters in the LVR group showed significant differences. In particular, the LVSP and $\pm dp/dt_{max}$ significantly decreased ($P < 0.01$), and the LVEDP significantly increased ($P < 0.01$) (Table 1).

Table 1. Changes in Hemodynamic Parameters

Group	n	LVSP (mmHg)	LVEDP (mmHg)	+dp/dt _{max} (mmHg/s)	-dp/dt _{max} (mmHg/s)
Sham-operated	11	132.87±2.89	4.84±0.52	4551.6±145.46	3643.9±204.36
LVR	12	110.1±4.51*	9.92±0.94*	2918.8±437.81*	2808.9±112.1*

Note. * $P < 0.01$, compared with the sham-operated group.

Pathological Changes in Myocardial Tissue

As shown by H-E staining, in the sham-operated group, the normal myocardial cells were arranged in an orderly manner, with carmine-colored nuclei and plum-colored cytoplasm. In the LVR group, however, myocardial fibrosis was obvious, with hyacinthine-colored collagen tissue; the surviving myocardial cells, which were irregularly arranged, were found in the border zones.

As shown by Masson staining, in the sham-operated group, the normal cardiac muscles were bright red and the cytoplasm was evenly stained. In the LVR group, the myocardial cells showed a diffuse

brick red cytoplasmic staining, with blue collagen tissue and obvious myocardial fibrosis (data not shown).

Proteomic Analysis

Proteomic analysis identified 808 proteins in the LVR group and 809 proteins in the sham-operated group, with inter-assay overlapping rates of 76.74% and 78.63%, respectively, indicating that the assay had good repeatability. Furthermore, a high-resolution mass spectrometer, the LTQ-Orbitrap, was used for proteomic analysis, and the mean error of polypeptide mass was 1.5 ppm (Table 2).

Table 2. Protein Identification in the LVR Group and the Sham-operated Group

Group	Run1	Run2	Run3	Total	Overlapping Proteins	Overlapping Rate
Sham-operated	608	640	609	809	475	76.74%
LVR	522	635	605	808	488	78.63%

Differential Proteomic Analysis

Using the spectrum count, semiquantitative differential proteomic analysis was performed. Twenty-one differentially expressed proteins were identified (Table 3). Compared with the sham-

operated group, 10 proteins were upregulated and four proteins were downregulated in the LVR group. Three proteins were found only in the LVR group, but not in the sham-operated group. Four proteins were found only in the sham-operated group, but not in the LVR group.

Table 3. Differentially Expressed Proteins in the LVR Group and the Sham-operated Group

Protein ID	Protein Name	Spectrum Count	
		Sham-operated	LVR
Upregulated Proteins in the LVR Group			
IPI: IPI00195372	Eef1a1 Elongation factor 1-alpha 1	3	43
IPI: IPI00421429	Jup Junction plakoglobin	17	44
IPI: IPI00959144	LOC363331 plasma membrane associated protein, S3-12	22	48
IPI: IPI00555287	Sptbn1 Non-erythroid spectrin beta	18	41
IPI: IPI00206403	Lum Lumican	7	25
IPI: IPI00189173	Ryr2 Ryanodine receptor 2	69	115
IPI: IPI00197555	Sucg1 Succinyl-CoA ligase [GDP-forming] subunit alpha, mitochondrial	58	96

(Continued)

Protein ID	Protein Name	Spectrum Count	
		Sham-operated	LVR
IPI:IPI00203054	Acsf2 Acyl-CoA synthetase family member 2, mitochondrial	42	65
IPI:IPI00210360	Hspg2 394 kDa protein	30	51
IPI:IPI00205745	Prdx5 Isoform Mitochondrial of Peroxiredoxin-5, mitochondrial	33	52
Downregulated Proteins in the LVR Group			
IPI:IPI00191112	Ndufab1 Acyl carrier protein	77	35
IPI:IPI00367152	Ndufv2 NADH dehydrogenase [ubiquinone] flavoprotein 2, mitochondrial	67	44
IPI:IPI00212767	Prss1 Anionic trypsin-1	168	108
IPI:IPI00198717	Mdh1 Malate dehydrogenase, cytoplasmic	320	187
Missing Proteins in the Sham Group			
IPI:IPI00569279	Hist2h2ab Histone H2A	0	182
IPI:IPI00954691	Hist2h2aa3;LOC690131 Histone H2A type 2-A	0	163
IPI:IPI00968501	IgG-2a Ig gamma-2A chain C region	0	51
Missing Proteins in the LVR Group			
IPI:IPI00895570	Putative uncharacterized protein	79	0
IPI:IPI00361346	IgG-2a LOC367586 protein	86	0
IPI:IPI00776957	Uncharacterized protein	168	0
IPI:IPI00201578	Myh3 Myosin-3	1151	0

Results of Western Blot Analysis

We validated two proteins by western blotting. The expression of *Eef1a1* was significantly increased

in LVR group ($P<0.01$). The expression of *JUP* was also increased in LVR group ($P<0.05$). (Figure 1). These results matched those found by comparative proteomics.

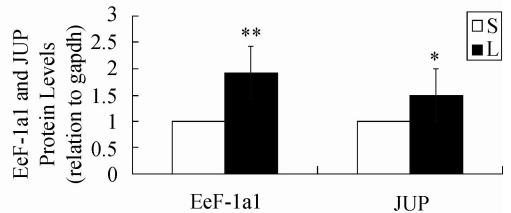
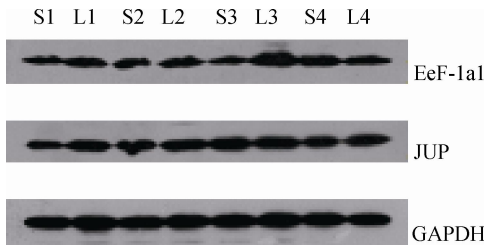


Figure 1. Western Blot analysis of *EeF1a1* and *JUP* in the LVR group (L) and sham-operated group (S). Left panel: Western blot showing immunoreactive bands for *EeF1a1* and *JUP* and the *GAPDH* control. Right panel: Graph of the western blot band intensities relative to *GAPDH*, determined by densitometric scanning. (** $P<0.01$, * $P<0.05$).

DISCUSSION

LVR following MI refers to the changes in the morphology and sizes of the infarction zone and non-infarction zone across the whole LV following AMI. LVR includes cellular reconstruction, which includes loss of myocardial cells, hypertrophy due to poor myocardial adaption, and fibrosis of the extracellular matrix. It can be divided into an early stage of infarct expansion and an advanced stage of global ventricular dilatation (GVD)^[12]. Myocardial

remodeling is the pathophysiological basis of heart failure, and can directly affect the prognosis of MI and heart failure.

Hypoxia and necrosis of myocardial cells in the blood supply area can occur after acute coronary artery occlusion. The necrotic cardiac muscle loses its systolic function, and the ischemic cardiac muscle displays weakened systolic function; the cardiac muscle in the non-diseased region has relatively normal function. The combined contraction of these three types of cardiac muscles will unavoidably

result in disordered or imbalanced systolic and diastolic functions, and in changes to hemodynamic parameters. In our study, the hemodynamic parameters of rats were significantly damaged four weeks after MI, which was consistent with a previous report^[13]. Hemodynamic changes are the cause of the compensatory hypertrophy of myocardial cells, and are also the results of hypertrophy of the myocardial cells. Thus, they form a vicious circle, and can cause GVD and heart failure.

Many studies have demonstrated that the pathological process of LVR following MI includes necrosis of myocardial cells, hypertrophy of non-necrotic myocardial cells, infiltration of inflammatory cells, development of granulation tissue, myofibrillar hyperplasia, and scar formation. The sections of cardiac muscle tissues in this experiment displayed all of the above pathological changes^[14]. These pathological changes are also the basis of infarct expansion of the heart and GVD, and of the decreased systolic and diastolic functions. They interact with the hemodynamic changes, and finally cause heart failure.

In this study, 21 differentially expressed proteins were identified, which could be divided into six categories based on their functions: 1) Protein synthesis-related proteins: Elongation factor 1- α 1 (Eef1 α 1), which binds GTP and aminoacyl-tRNA forming a ternary complex and is responsible for the enzymatic delivery of aminoacyl-tRNAs to the A site of the ribosome. Zhang et al. found abnormal Eef1 α 1 expression in rats with acute myocardial ischemia^[15]. However, a similar result was not found in rats with myocardial remodeling and/or heart failure. 2) Cytoskeletal proteins: as a cell junction protein, junction plakoglobin (Jup) is a major component participating in cell-cell adhesion in junctions and is a main component of the desmosomal plaque complex. The desmosome is mainly involved in the conduction of mechanical stress, causing synchronous contraction of the cardiac muscle. Another study demonstrated that variations in genes and proteins were associated with arrhythmogenic right ventricular cardiomyopathy^[16]. Non-erythroid spectrin beta (Sptbn1) is also an actin crosslinking and molecular scaffold protein. Myosin-3 (Myh3), myosin heavy chain (MHC), and myosin light chains (MLC1/MLC2) can bind to generate functional contraction. Merry et al. found that the expression of myosin increased in transverse aortic constriction rat models with myocardial hypertrophy^[17]. In our experiment, the expression of MHC3 was negative during myocardial

remodeling, which is considered to be related to the different subtypes and different stages of heart failure. 3) Channel proteins: Ryanodine receptor 2 (RyR2) is the main Ca²⁺ release channel in the sarcoplasmic reticulum of myocardial cells, and has a key role in the excitation-contraction coupling of cardiac muscles. The influx of a small amount of calcium into the cytoplasm leads to the opening of cardiac sarcoplasmic reticulum (SR) calcium release channel (RyR2), causing a massive release of calcium ions. This results in the formation of a cross bridge between actin and myosin, movement of tropomyosin, and contraction of myofilaments. However, the role of RyR2 in the development of heart failure remains controversial. In an experimental dog model of chronic HF, Zuzana et al.^[18] found decreased contractility and diminished SR Ca release characteristic of failing myocardium, which could be explained by increased sensitivity of RyR2 to luminal Ca, leading to enhanced spark-mediated SR Ca leak and reduced intra-SR Ca²⁺. Takeshi et al. analyzed the affinity of the high-affinity binding site of Ryanodine in hamster models with cardiomyopathies^[19]. They found that the affinity was not significantly different in the early stage (weeks 8 and 18) between the cardiomyopathy group and control group, and decreased significantly only in the late stage (week 28). Quantitative immunoprecipitation analysis showed that the amount of RyR2 protein increased in the early stage in the cardiomyopathy group and decreased below the normal level after the occurrence of heart failure. 4) Energy metabolism-related proteins: Succinyl-CoA ligase [GDP-forming] subunit alpha, mitochondrial (Succ1g1). This enzyme is targeted to the mitochondria and catalyzes the conversion of succinyl CoA and ADP or GDP to succinate and ATP or GTP. This is a substrate level phosphorylation process in the tricarboxylic acid cycle. Acyl-CoA synthetase family member 2, mitochondrial (Acsf2) catalyzes the initial reaction of fatty acid metabolism to produce acyl-coenzyme A for further oxidation of fatty acid β . NADH dehydrogenase [ubiquinone] flavoprotein 2, mitochondrial (Ndufv2) participates in electron transport in the respiratory chain. Malate dehydrogenase, cytoplasmic (Mdh1) facilitates the dehydrogenation of hydroxysuccinic acid into ketosuccinic acid in the tricarboxylic acid cycle. During heart failure, energy metabolism becomes disordered and its mode is transformed, as has been demonstrated in many studies^[20]. 5) Anti-oxidation-related proteins: Mitochondrial isoform of peroxiredoxin-5 (Prdx5) is a member of

the peroxidase family, and is able to catalyze and decompose H₂O₂ and lipid peroxides, clear excessive active oxygen, and protect cardiac muscles.

6) Immune-related proteins: Ig gamma-2A chain C region (IgG-2a) can bind to antigens and produce an immune reaction. There is speculation that immune reactions may also have a role in LVR. The remaining proteins were of unknown or unclear functions and these may also have roles in myocardial remodeling. Their functions require further research.

In this study, after establishing an animal model of LVR following MI, we analyzed the hemodynamics, pathology, and differential proteomics of LVR. The hemodynamic and pathological changes are the bases of LVR and heart failure. We identified 21 differentially expressed proteins using differential proteomic techniques. These findings provide clues to the pathophysiological mechanisms of LVR, and may help in identifying new drug targets for the prevention and treatment of LVR.

REFERENCES

1. Onodera H, Matsunaga T, Tamura Y. Enalapril suppresses ventricular remodeling more effectively than losartan in patients with acute myocardial infarction. *Am heart J*, 2005; 150, 689-94.
2. Sabbah HN. Ventricular Remodeling. *Ann Med*, 1998; 30 (suppl), 32-5.
3. Palojoki E, Saraste A, Erikason A, et al. Cardiomyocyte apoptosis and ventricular remodeling after myocardial infarction in rats. *Am J Physiol Heart Circ Physiol*, 2001; 280(6), H2726-31.
4. Wasinger VC, Cordwell SJ, Cerpa PA, et al. Progress with gene-product mapping of the mollicutes *Mycoplasma genitalium*. *Electrophoresis*, 1995; 16(7), 1090-4.
5. Agnetti G, Kane LA, Guarnieri C, et al. Proteomic technologies in the study of kinases novel tools for the investigation of PKC in the heart. *Pharmacol Res*, 2007; 55(6), 511-22.
6. Pinet F. Proteomics in cardiology. *Arch Mal Coeur Vaiss*, 2007; 100 (1), 47-51.
7. Ouzounian M, Lee DS, Gramolini AO, et al. Predict prevent and personalize genomic and proteomic approaches to cardiovascular medicine. *Can J Cardiol*, 2007; 23(SupplA), 28A-33A.
8. Buscemi N, Doherty KA, Sussman MA, et al. Proteomic analysis of Racl transgenic mice displaying dilated cardiomyopathy reveals an increase in creatine kinase M-chain protein abundance. *Mol Cell Biochem*, 2003; 251(1-2), 145-51.
9. Weekes J, Wheeler CH, Yan JX, et al. Bovine dilated cardiomyopathy: Proteomic analysis of an animal model of human dilated cardiomyopathy. *Electrophoresis*, 1999; 20(4-5), 898-906.
10. Tao ZW, Huang YW, Xia Q, et al. Early association of electrocardiogram alteration with infarct size and cardiac function after myocardial infarction. *J Zhejiang Univ Sci*, 2004; 5, 494.
11. Bradford MM. A rapid and sensitive method for the quantitation of microgram quantities of protein utilizing the principle of protein-dye binding. *Anal Biochem*, 1976; 72, 248-54.
12. Mitchell GF, Lamas GA, Vaughan DE, et al. Left ventricular remodeling in the year after first anterior myocardial infarction: a quantitative analysis of contractile segment lengths and ventricular shape. *J Am Coll Cardiol*, 1992; 19(6), 1136-44.
13. Mann DL. Mechanisms and models in heart failure. *Circulation*, 1999; 100(9), 999-1008.
14. Wenyuan Zhao. Temporal and spatial characteristics of apoptosis in the infarcted rat heart. *Biochem Biophys Res Commun*, 2004; 325, 605-11.
15. Zhang GQ. Time Course Proteomic Profile and Differentially Expressed Genes of Rat Acute Myocardial Ischemia. Doctor Dissertation, Sichuan Univ, Chengdu, 2007.
16. Mckoy G, Protonotarios N, Crosby A, et al. Identification of a deletion in plakoglobin in arrhythmogenic right ventricular cardiomyopathy with palmoplantar keratoderma and woolly hair(Naxos disease). *Lancet*, 2000; 355, 2119-24.
17. Lindsey ML, Goshorn DK, Comte Walters S, et al. A multidimensional proteomic approach to identify hypertrophy associated proteins. *Proteomics*, 2006; 6, 2225-35.
18. Zuzana K, Dmitry T, Serge V, et al. Abnormal intrastore calcium signaling in chronic heart failure. *Proc Natl Acad Sci USA*, 2005; 102(39), 14104-9.
19. Takeshi U, Tomoko O, Yuji H, et al. Alterations in cardiac SR Ca²⁺-release channels during development of heart failure in cardiomyopathic hamsters. *Am J Physiol Heart Circ Physiol*, 1998; 274, 1-7.
20. Zhou SG, Zhou SF, Huang HQ, et al. Proteomic analysis of hypertrophied myocardial protein patterns in renovascularly hypertensive and spontaneously hypertensive rats. *J Proteome Res*, 2006; 5, 2901-8.